

## Shape- and size-controlled synthesis of noble metal nanoparticles

Kyeong Woo Choi<sup>1a</sup>, Do Youb Kim<sup>2b</sup>, Seong Ji Ye<sup>1a</sup>, and O Ok Park<sup>\*1</sup>

<sup>1</sup>*Department of Chemical and Biomolecular Engineering (BK21+ graduate program), Korea Advanced Institute of Science and Technology (KAIST), 291 Daehakro, Yuseong-gu, Daejeon 305-701, Republic of Korea*

<sup>2</sup>*Advanced Materials Division, Korea Research Institute of Chemical Technology (KRICT), 141 Gajeongro, Yuseong-gu, Daejeon 305-600, Republic of Korea*

*(Received June 16, 2014, Revised November 25, 2014, Accepted December 16, 2014)*

**Abstract.** Noble metal nanoparticles (mainly Au, Ag, Pt and Pd) have received enormous attention owing to their unique and fascinating properties. In the past decades, many researchers have reported methods to control the shape and the size of these noble metal nanoparticles. They have consequently demonstrated outstanding and tunable properties and thus enabled a variety of applications such as surface plasmonics, photonics, diagnostics, sensing, energy storage and catalysis. This paper focuses on the recent advances in the solution-phase synthesis of shape- and size-controlled noble metal nanoparticles. The strategies and protocols for the synthesis of the noble metal nanoparticles are introduced with discussion of growth mechanisms and important parameters, to present the general criteria needed for producing desirable shapes and sizes. This paper reviews their remarkable properties as well as their shape- and size- dependence providing insights on the manipulation of shape and size of metal nanoparticles, necessary for appropriate applications. Finally, several applications using the shape- and size-controlled noble metal nanoparticles are highlighted.

**Keywords:** metal nanoparticles; size and shape; growth mechanism; properties; applications

---

### 1. Introduction

Throughout human history, metals, which cover more than two thirds of the elements, have been an important and necessary material in a variety of fields. Nowadays, the characteristics of metallic materials can be modified due to nanotechnology, and their properties can be dramatically changed by altering their large surface-to-volume ratio, and confinement of electromagnetic components (Sau 2009). As a result, nano-sized metal particles exhibit unique and outstanding physical, chemical, electrical, optical and catalytic properties compared to their bulk counterparts (Burda 2005, Wilcoxon 2006, and Daniel 2004). Because of these remarkable properties, metal

---

\*Corresponding Author, Professor, E-mail: [ookpark@kaist.ac.kr](mailto:ookpark@kaist.ac.kr)

<sup>a</sup>Ph.D. Student

<sup>b</sup>Ph.D.

nanoparticles are considered to be promising materials for use in plasmonics, diagnostics, sensing, energy storage and catalysis (Lu 2009, Rosi 2005, and Aricò 2005).

It is worth pointing out that the properties of metal nanoparticles are highly dependent on the size and shape of the nanoparticles (Aiken III 1999 and Somorjai 1985). Therefore, controlling the size and the shape of the metal nanoparticles has been a very significant research focus because such methods allow the fine tuning of their properties. This paper is focused on the recent advances in the solution-phase synthesis of size- and shape-controlled noble metal nanoparticles. In the recent decades, strategies and protocols for the preparation of size- and shape-controlled metal nanoparticles have been eagerly reported, such as spheres, octahedra, cubes, cuboctahedra, rods, wires, decahedra, icosahedra, and plates (Xia 2009 and Tao 2008). Moreover, even shapes not thermodynamically favored beyond the conventional polyhedrons are often synthesized, including high-index facets, concave surfaces, and branched structures. (Zhang 2012 and Lim 2010).

Despite various synthetic protocols, however, it is still difficult to design and prepare metal nanoparticles with the desired size and shape because their detailed chemistries and growth mechanisms are very complicated. There is ongoing current research on the growth mechanisms of size- and shape-controlled metal nanoparticles, which seeks to establish general understandings of the various chemicals and structures needed to obtain the desirable metal nanoparticles. Such discussions will be presented in this paper by reviewing several strategies and preparations of size- and shape-controlled metal nanoparticles that have been performed in our own research group.

In addition, the synthesis of metal nanoparticles with well-controlled size and shape has allowed investigation of their remarkable properties, as well as their size- and shape-dependence. Such studies offer insights into the relation between the manipulation of shape and size of the metal nanoparticles and their properties, and specifically, their relation to appropriate applications. In this regard, several possible applications using the shape- and size-controlled metal nanoparticles are introduced with actual examples, including our experimental results.

## **2. Synthesis of metal nanoparticles**

Thanks to an enormous range of research, a variety of routes to synthesize metal nanoparticles have been presented to date, including template-directed growth (Jana 2001), electrochemical synthesis (Tian 2007), photochemical synthesis (Jin 2001), solvothermal synthesis (Dutilleul 2014) and solution phase synthesis. Among them, synthesis approaches based on a solution phase reduction possess many remarkable advantages compared to other methods. These include 1) simplicity and cost effectiveness, 2) flexibility in controlling reaction parameters, 3) easy surface modification and additional treatment, and 4) the possibility of mass production. In solution phase synthesis, metal nanoparticles are formed by the reduction of metal ions with a reducing agent and a surfactant/capping agent in the solution mixture. The formation of metal nanoparticles basically involves nucleation and growth mechanisms (LaMer 1950), however, the research into the details of those mechanisms is still ongoing, with the intent of routinely obtaining metal nanoparticles with well-defined size and shape.

One of the preferred synthetic strategies to obtain size- and shape-controlled metal nanoparticles is the seed-mediated growth method. The seed-mediated growth method is a two-step synthesis of metal nanoparticles, divided into preparation of the seeds and their subsequent growth (Jana 2001). This method offers greater flexibility in controlling both the size

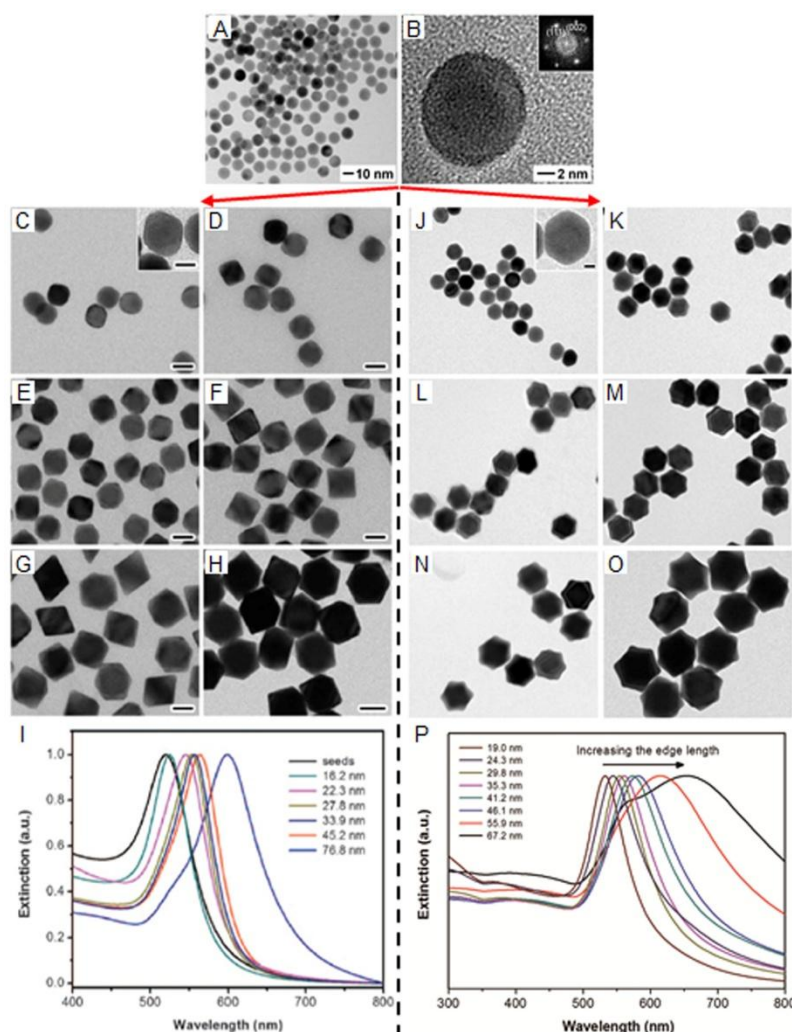


Fig. 1 (A) TEM image of single-crystal Au nanospheres used as seeds and (B) HRTEM image of an individual Au seed and the corresponding FFT pattern (inset) (Reproduced with permission from ref. Choi 2013, copyright 2013 Royal Society of Chemistry). (C-H) TEM images of Au octahedra with different edge lengths and (I) their UV-vis extinction spectra (Reproduced with permission from ref. Kim 2011, copyright 2011 Wiley-VCH). (J-O) TEM images of Au rhombic dodecahedra with different edge lengths and (P) their UV-vis extinction spectra (Reproduced with permission from ref. Choi 2013, copyright 2013 Royal Society of Chemistry)

and the shape of the resultant metal nanoparticles (Sau 2004). Since the nucleation stage is separated from the growth stage, the resultant shape of the metal nanoparticles can be conventionally controlled by using different types of crystalline structure (*e.g.* single crystal vs. multiply twinned particle), and/or by applying different reaction conditions (*e.g.* reactant species, reactant concentration, reaction temperature) during the growth (Ma 2010). The size distribution of the resultant metal nanoparticles can often be improved through a “self-focusing” mechanism (Peng 1998). Moreover, it generally requires a milder reaction conditions compared to a

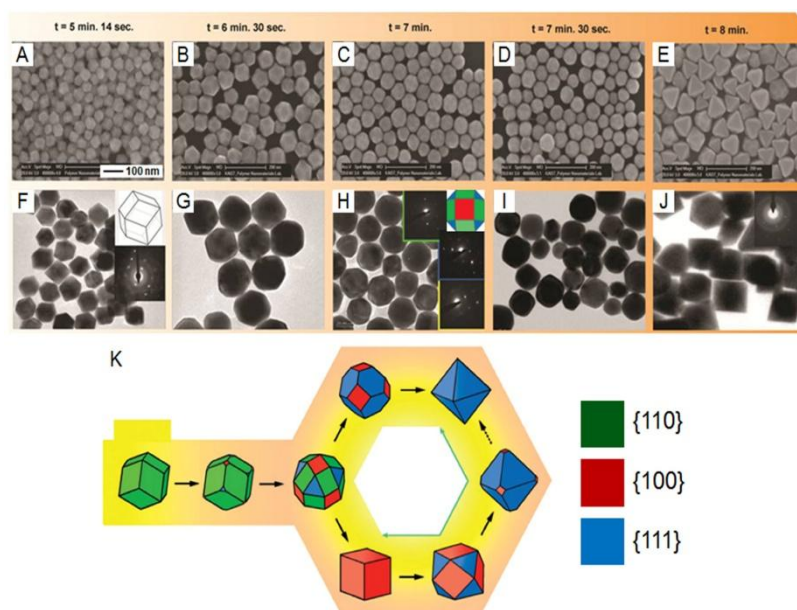


Fig. 2 (A-E) SEM images of Au nanoparticles transformed from rhombic dodecahedra to rhombicuboctahedra and to octahedra and (F-J) the corresponding TEM images as a function of reaction time. (K) A schematic illustration for the shape transformation of Au nanoparticles. The red, blue, and green colors represent the {100}, {111}, and {110} facets, respectively (Reproduced with permission from ref. Kim 2010, copyright 2013 Royal Society of Chemistry).

self-nucleation process (Qiu 2009). The synthesis of Au octahedra and Au rhombic dodecahedra with well-defined sizes and shapes *via* seed-mediated growth method has been also demonstrated, as shown in Fig.1 (Kim 2011 and Choi 2013). Starting from single-crystal seeds of Au nanospheres with a uniform sizes (Fig. 1A and 1B), it is possible to reproducibly obtain Au octahedral and Au rhombic dodecahedra with a narrow size distribution and in high percentages. Their size can be readily controlled in a relatively broad range by varying the amount of the seeds, the concentration of  $\text{HAuCl}_4$ , or both (Fig. 1C-H and Fig. 1J-O). In addition, the optical properties, represented by the localized surface plasmon resonance peak, could be finely tuned in a wide range of visible light (Fig. 1I and 1P).

### 3. Shape-control of metal nanoparticles

Depending on the nucleation and growth mechanisms, metal atoms reduced from metal ions will subsequently aggregate with each other and form nuclei. Then, the nuclei continuously grow into nanoparticles having several possible shapes, which can be determined by the initial crystalline structures. For example, a single crystal can evolve into an octahedron, cuboctahedron, cube, or octagonal rod (Seo 2006 and Xiong 2007) whereas the multiply twinned particle can evolve into a decahedron, icosahedron, or five-fold twinned rod (Seo 2008 and Ni 2005). During growth, the nanoparticles usually grow in the manner of thermodynamically favored pathways to minimize their total surface energy (Xiong 2007). In the case of a metal with a fcc structure, the

surface energy of each facet increases in the order of  $\{111\} < \{100\} < \{110\}$  for low-index facets (Wang 2000). As a result, the metal nanocrystals tend to be evolved into the shapes with surface exposed by  $\{111\}$ ,  $\{100\}$ , or a mix of both  $\{111\}$  and  $\{100\}$  facets to minimize total surface energy (Marks 1994), while other facets with high surface are disappear. It has been also demonstrated that such a shape evolution of metal nanoparticles can be obtained experimentally, as shown in Fig. 2 (Kim 2010). The Au rhombic dodecahedra at the initial stage of the reaction were continuously transformed through the rhombicuboctahedron to a cube or a cuboctahedron, and then to an octahedron or a truncated octahedron. In order to control the shape of the resultant metal nanoparticles, therefore, the passivation of desired facets and/or manipulation of the growth rate for each direction, such as the  $[111]$ ,  $[100]$ , and  $[110]$  directions, is required.

### 3.1 Surface capping

One way to control the final shape of metal nanoparticles is with the introduction of a capping agent. The capping agents or similar impurities can selectively interact with certain surfaces of the metal nanoparticles and thus change the order of free energies of different facets (Pimpineli 1998). This is highly related with the relative growth rates along the different directions. The facet with a higher growth rate along its perpendicular direction easily disappears during the growth while the facet having a lower growth rate will survive and be exposed on the metal nanoparticle surface (Seo 2006). For example, poly vinyl(pyrrolidone) (PVP), a popular polymeric capping agent, is often used to stabilize  $\{100\}$  facets of Ag (Sun 2003). Bromide ion, which can play a role as an ionic capping agent, is selectively adsorbed onto the  $\{100\}$  facets of various noble metals, to

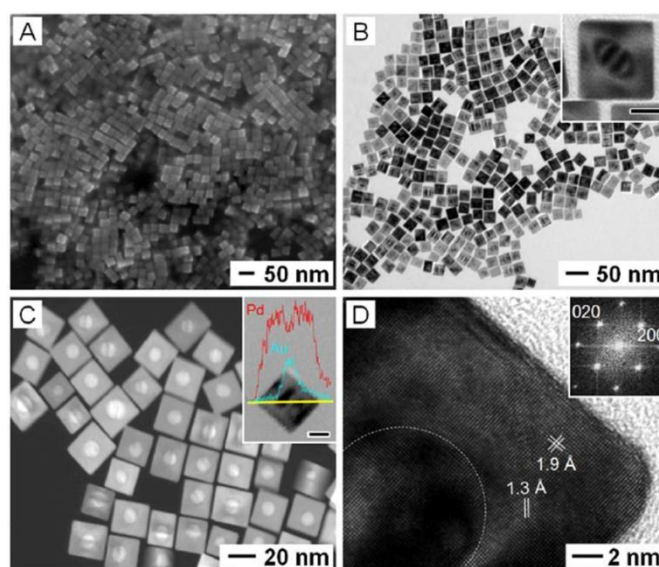


Fig. 3 (A) SEM image and (B) TEM image of the Au@Pd core-shell nanocubes. (C) HAADF-STEM image of the Au@Pd core-shell nanocubes and TEM image with cross-sectional composition line-profile (inset). (D) HRTEM image taken from part of an individual Au@Pd core-shell nanocube and the corresponding FFT pattern (inset) (Reproduced with permission from ref. Kim 2013, copyright 2013 Royal Society of Chemistry)

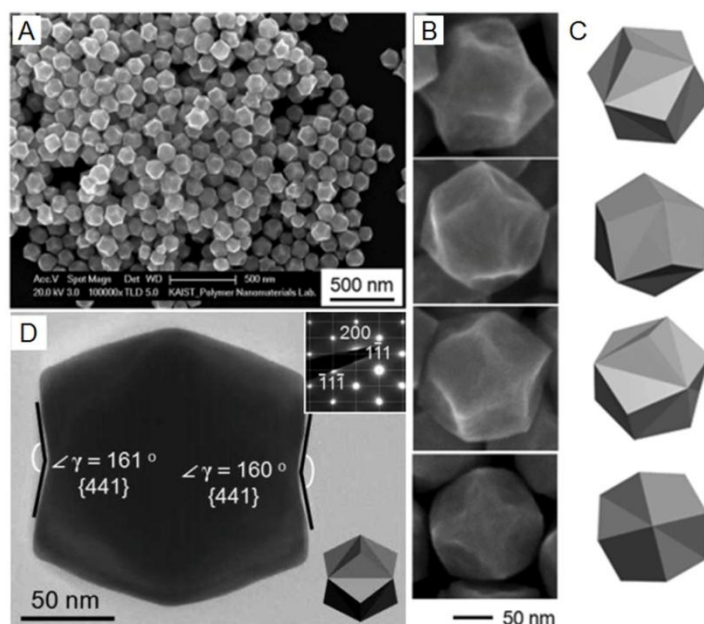


Fig. 4 (A) Low-magnification SEM image of Au trisoctahedra. (B) High-magnification SEM images of Au trisoctahedra in four different orientations and (C) schematics of trisoctahedra that correspond to the obtained nanoparticles in (B) in the same orientation. (D) TEM image of a single as-prepared Au trisoctahedron recorded along the [011] directions and the corresponding SAED pattern (inset) (Reproduced with permission from ref. Kim 2012, copyright 2012 Techno Press)

generate nanocubes and nanobars, which are enclosed only by {100} facets (Xiong 2007). In a recent study, it has been reported that Au@Pd nanocubes with uniform and controllable sizes could be synthesized by employing an ionic surfactant, cetyltrimethylammonium bromide (CTAB) (Kim 2013). Fig. 3 shows the SEM and TEM images of the obtained Au@Pd core-shell nanocubes, with highly uniform size and shape. The high-angle annular dark-field scanning TEM (HAADF-STEM) image and the HRTEM image (Fig.3C and 3D) confirm the spherical Au seed and Pd shell which was grown in an epitaxial manner and exposed with {100} facets. The bromide ion in CTAB adsorbed onto the {100} facets, generating the Pd shell, and thus Au@Pd nanocubes were formed. When citrate was used for the Pd nanoparticles, the citrate ions tend to bind most strongly to the {111} facets of Pd and thus Pd octahedra, icosahedra, and decahedra, which are enclosed only by {111} facets, can be prepared (Lim 2007).

### 3.2 Underpotential deposition

Underpotential deposition (UPD) is the electrodeposition of metal monolayer(s) on a foreign metal substrate at potentials that can be significantly less negative than is possible for deposition on the same metal surface as the adsorbate (Herrero 2001). The UPD can be also adopted to synthesize size- and shape-controlled metal nanoparticles. For example, Ag ions have been widely used for the preparation of shape-controlled Au nanocrystals by UPD; the ions hinder newly formed Au atoms from being nucleated and grown on the Au surfaces covered with Ag

(Orendorff 2006). It is possible to obtain shape-controlled Au nanoparticles with 24  $\{hhl\}$  high-index facets, Au trisoctahedra *via* UPD (Kim 2012). Fig. 4A shows a typical SEM image of as-prepared Au trisoctahedra. The obtained Au trisoctahedra were well-matched with the schematics of ideal trisoctahedra in different orientations (Fig. 4B and 4C). The Ag ions in the reaction solution played a critical role in controlling the trisoctahedral shape of the resultant Au nanoparticles produced by UPD on the Au surfaces. The HRTEM image confirms that the as-prepared Au trisoctahedra were single crystal and enclosed by high-index facets, including  $\{441\}$ ,  $\{773\}$ , and  $\{331\}$  (Fig. 4D).

### 3.3 Kinetically controlled reaction

In recent studies, new synthetic protocols have suggested a different approach to control the shape of metal nanoparticles, namely, the kinetically controlled reaction. It concerns the manipulation of the growth rate at which the metal atoms are generated and added to the surface of a growing nanoparticle (Zhang 2012). Typically, if the reduction rate is considerably slow, a kinetically controlled reaction can be achieved (Sun 2003). The kinetically controlled reaction can be driven by the following conditions: 1) substantially slowing down the reduction or the formation rate of atoms (Xiong 2007); 2) using a considerably weak reducing agent (Washio 2006); 3) coupling the reduction to an oxidation process (Xiong 2005); and/or 4) inducing Oswald ripening (Sun 2003). The products generated by the kinetically controlled reaction may take thermodynamically unfavorable shapes containing concaved surfaces, high-index facets, and branched structures (Zhang 2012 and Lim 2010).

For example, shape-controlled Au nanocrystals with  $\{hk0\}$  high-index facets were synthesized by controlling the reduction rate (Kim 2010). Fig. 5A and 5B shows the as-prepared Au

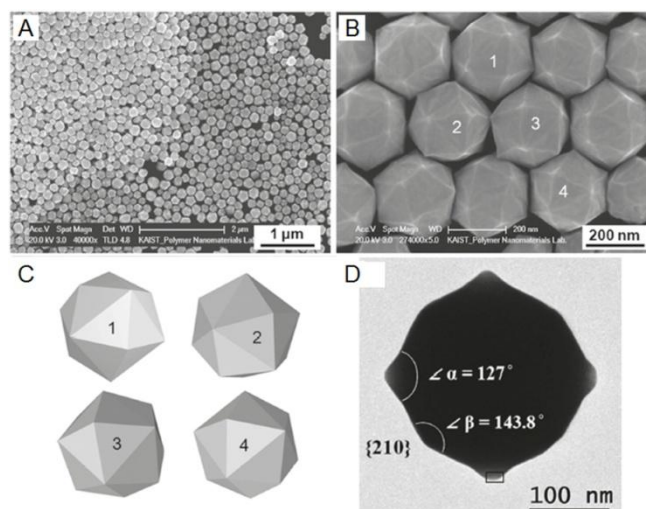


Fig. 5 (A) Low-magnification and (B) high-magnification SEM images of Au tetrahexahedra. (C) Schematics of a tetrahexahedron in four different orientations that correspond to those of nanoparticles marked with the same numbers in (B). (D) TEM image of a single as-prepared Au tetrahexahedron recorded along the  $[001]$  directions (Reproduced with permission from ref. Kim 2010, copyright 2010 American Chemical Society)

tetrahexahedra with well-defined shape. Fig. 5C is the schematic of a tetrahexahedron in four different orientations, which were well-fitted with the obtained Au nanocrystals marked with the numbers in Fig. 5B. Since  $\text{HAuCl}_4$  was reduced by *N,N*-dimethylformamide (DMF), which is a relatively weak reducing agent, and a high concentration of PVP was used, the reduction rate became considerably slow. As a result, high-index facets such as  $\{210\}$  facets have survived and are exposed at the surface of the Au nanoparticles, and thus tetrahexahedral (THH) Au nanoparticles, which are bounded by 24  $\{210\}$  facets (Fig. 5D), were synthesized.

The reduction rate could be also controlled by choosing an appropriate surfactant. It was reported that Au@Pd nanocubes with concaved surfaces rather than flat surfaces could be generated when CTAB was replaced by cetyltrimethylammonium chloride (CTAC) in the reaction system (Li 2012). It was speculated that the increased reduction rate in the CTAC system relatively accelerated the Pd growth on the corner site of the seed and reduced Pd atoms were restricted from migrating to the edges and side surfaces due to the rapid drop of reduction rate by the quick consumption of Pd ions. As a similar approach, if one introduces a surfactant which can accelerate the directional growth of Pd on the Au seed and stabilize the formed Pd between each other, Au@Pd nanoparticles with opened shell structure can be synthesized (Kim 2013) (Fig. 6). Indeed, when cetylpyridinium chloride (CPC) containing the chloride anion group, long alkyl chain, and rigid pyridinium group was used as a surfactant, the flower-like Au@Pd nanostructures could be

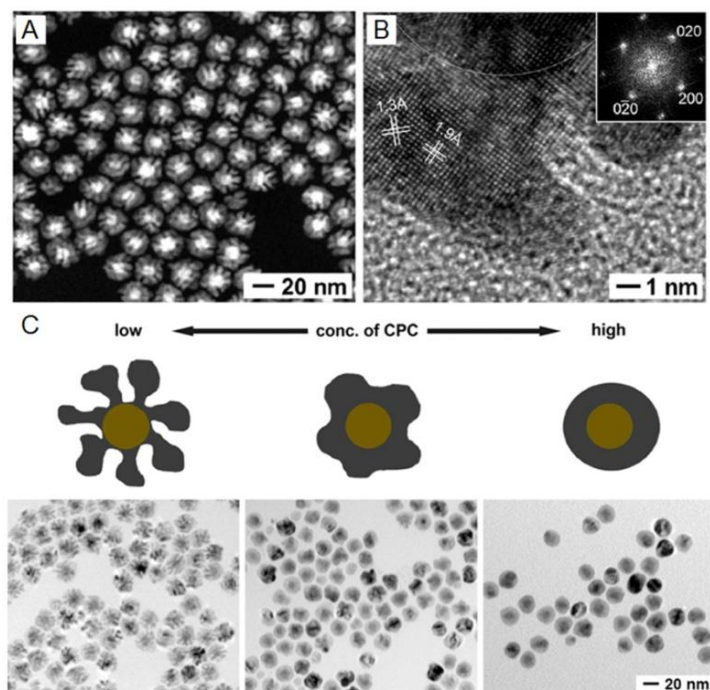


Fig. 6 (A) HAADF-STEM image of the flower-like Au@Pd nanostructures. (B) HRTEM image taken from part of a flower-like Au@Pd nanostructure and the corresponding FFT pattern (inset). (C) Schematic illustration of the shape changes of Au@Pd nanostructures as a function of the concentration of CPC and the corresponding TEM images (Reproduced with permission from ref. Kim 2013, copyright 2013 Royal Society of Chemistry).

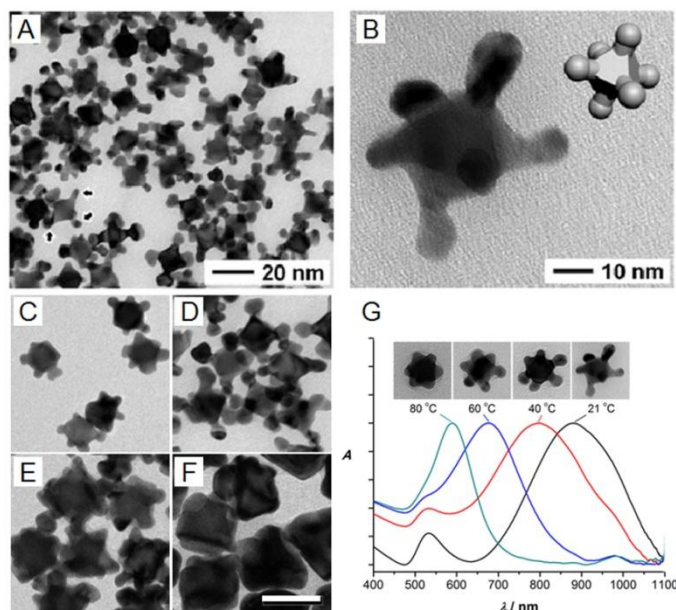


Fig. 7 (A) Low-magnification TEM image of Au nano-hexapods and (B) high-magnification TEM image of a single Au nano-hexapod with its schematic drawing proposed in the same orientation (inset). (C) TEM images of Au nanoparticles with different concentration of  $\text{HAuCl}_4$  (scale bar: 50 nm). (D) UV-vis extinction spectra of Au nano-hexapods of different arm lengths with the corresponding TEM images (Reproduced with permission from ref. Kim 2011, copyright 2011 Wiley-VCH).

prepared (Fig. 6A). The HRTEM image in Fig. 6B shows the opened nanostructure of a Pd shell on spherical Au seeds. The shape of the Pd shell can be controlled by changing the concentration of CPC (Fig. 6C). As the concentration of CPC increased, the Pd shell with opened nanostructure was gradually closed and eventually changed to a near-spherical shape with a smooth surface. This can be attributed to the different reduction kinetics of Pd caused by different concentrations of CPC. When the concentration of CPC was increased, the reduction rate of Pd precursor reduced, leading to the conformal overgrowth of Pd, and thus the completely closed core-shell nanostructure.

Adopting the kinetically controlled reaction conditions to seed-mediated growth, it is possible to design even more fascinating shapes with excellent properties, such as nano-hexapods (Kim 2011). A facile synthesis of Au nano-hexapods *via* seed-mediated growth in the presence of octahedral Au seeds has been reported under the kinetically controlled reaction (Fig. 7). The additional Au atoms are preferentially grown on the six vertices of the Au octahedral core, leading to the formation of Au nano-hexapods (Fig. 7B). A remarkably slow reduction rate could be induced by using a significantly low concentration of the additional precursor, weak reducing agent with low concentration (DMF, ca. 10% v/v), and a relatively low reaction temperature (room temperature). The obtained Au nano-hexapods had a well-defined shape, as well as uniform and controllable sizes, by adjusting their arm lengths (Fig. 7C–F and Fig. 7G). Because of their arms with controllable lengths, the Au nano-hexapods exhibited outstanding optical properties, which can be manipulated from the visible to the near-infrared region (Fig. 7G).

### 3.4 Particle attachment

Particle attachment can occur when relatively small particles collide with each other due to their higher surface energy and vigorous mobility (Zheng 2009 and Banfield 2000). According to the particle attachment growth mechanism, small particles generated at the early stage of the reaction coalesce into seeds, and those remaining, which were not consumed into the seeds, would freely diffuse and attach to the seeds after all, reducing their high surface energy (Lim 2010). Growth based on the particle attachment mechanism is often predicted to generate nanoparticles with dendritic shapes (Vicsek 1992). It is believed that the synthesis of the chestnut-bur-like Pd nanoparticles shown in Fig. 8 can be also described by the particle attachment mechanism (Ye 2014). The chestnut-bur-like Pd nanoparticles had a highly opened nanostructure and dozens of needle-like thin arms stretched outward (Fig. 8B). It is worth pointing out that the obtained Pd nanostructures were poly-crystalline containing several stacking faults (Fig. 8C). This indicates that the chestnut-bur-like Pd nanostructures were grown by the particle attachment growth mechanism. Fig. 8D-G, showing the time evolution of the Pd nanostructures, also supports that speculation. The Pd nanostructure appeared in the initial stage of the reaction (Fig. 8D) and gradually developed into chestnut-bur-like shape (Fig. 8E-G), while the small Pd agglomerates in the initial stage steadily decreased and finally disappeared (Fig. 8G). Considering the frequent stacking faults and the arm thickness of the chestnut-bur-like Pd nanostructures together with the size of Pd particles observed during the reaction, the chestnut-bur-like Pd nanostructures grew *via* particle attachment.

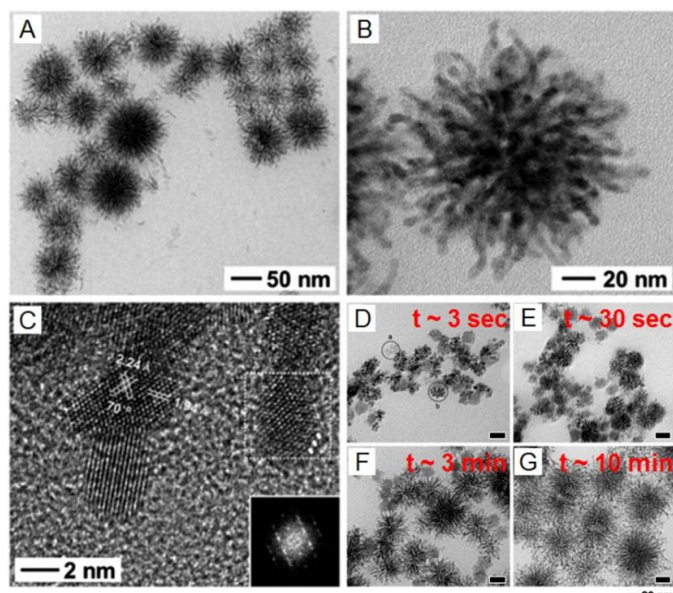


Fig. 8 (A) Low-magnification TEM image of Pd nanostructures and (B) high-magnification TEM image of a single Pd nanostructure. (C) HRTEM image taken from the apex of a single Pd nanostructure and the corresponding FFT pattern for the boxed area. (D) TEM images of Pd nanostructures obtained by quenching in the middle of the reaction, as a function of reaction time. (Reproduced with permission from ref. Ye 2014, copyright 2014 Royal Society of Chemistry)

## 4. Applications of metal nanoparticles

Successful synthesis of gelatin-co-PVA copolymer and the grafting of acrylic acid onto the copolymer have been carried out respectively by mutual and pre-irradiation methods. The grafted and the pristine copolymers have been characterized using different techniques. Both the copolymers have excellent swelling properties as those of superabsorbent hydrogel with good water retention properties. The copolymers have been used as a matrix for loading povidone, an antiseptic, for use as a wound dressing material and it was observed that the grafted samples have better healing properties than the pristine copolymer. Therefore, it can be concluded that  $\gamma$ -ray cross-linked gelatin-PVA hydrogels can be promising material for tissue engineering applications, it can be useful in delivering drug or nutrient or growth factors directly to the wound site by putting a swab over the hydrogel without removing the hydrogel from the wound site.

### 4.1 Optical and optoelectronic applications

When light irradiates a metal nanoparticle, the free electrons of the metal nanoparticle collectively oscillate in phase with the incident light and the induced charges are confined on the particle surface: this phenomenon is called localized surface plasmon resonance (LSPR) (Kelly 2003). Because of LSPR, Au and Ag nanoparticles can absorb and/or scatter a certain wavelength of light, which enables various optical applications (Jain 2006 and Wiley 2006). In addition, the particular wavelength of light with which metal nanoparticles interact can be adjusted through the size- and shape-control of the metal nanoparticles as mentioned above. LSPR can also enhance the local electric field around a metal nanoparticle and thus metal nanoparticles can be applied in a near-field enhancement, such as surface enhanced Raman scattering (SERS) (Kenipp 2007). Since

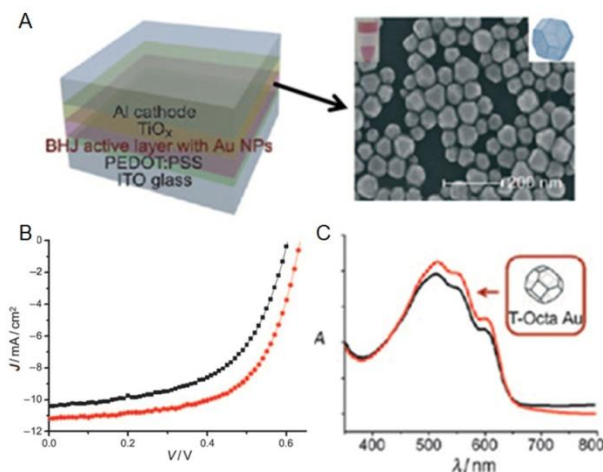


Fig. 9 (A) A schematic of a photovoltaic device containing Au nanoparticles in the active layer and SEM image of employed Au nanoparticle. (B) J-V curves of plain P3HT/PC70BM bulk-heterojunction devices (black) and those with 5 wt% Au nanoparticles (red). (C) UV/vis spectra of plain P3HT/PC70BM bulk-heterojunction films (black) and those with 5 wt% Au nanoparticles (red), thermally annealed at 150 °C for 20 min. (Reproduced with permission from ref. Wang 2011, copyright 2011 Wiley-VCH)

the Au and Ag have such fine optical properties as well as the advantage of easy surface modification, they are considered a remarkable candidate for the SERS substrate (Wang 2013 and Rycenga 2011). Therefore, many investigations are being conducted in order to perform reliable analysis and gain enhanced optical signals, such as the fabrication of a shape-controlled Au nanoparticles array on a nano-pattern.

Au nanoparticles can be also used in opto-electronic devices, such as electroluminescence and photovoltaics. In order to prevent exciton quenching by nonradiative energy transfer, Au nanoparticles have been generally located apart from an active layers. In principle, however, Au nanoparticles in the active layer can offer the possibility of enhanced light absorption, reduced cell resistance, and the synergistic effect of LSPR. The positive effects of Au nanoparticles in the active layer have been demonstrated by mixing Au nanoparticles with the active materials directly and coating them as a film on the cell (Wang 2011) (Fig.9A). The power conversion efficiencies of donor-acceptor polymer bulk-heterojunction solar cells were fairly enhanced for the various active materials including P3HT/PC70BM (Fig. 9B). It is believed that light absorption of the active layer was enhanced because of light scattering caused by the Au nanoparticles (Fig. 9C). Charge transport could be also improved due to the decrease of series resistance by Au nanoparticles.

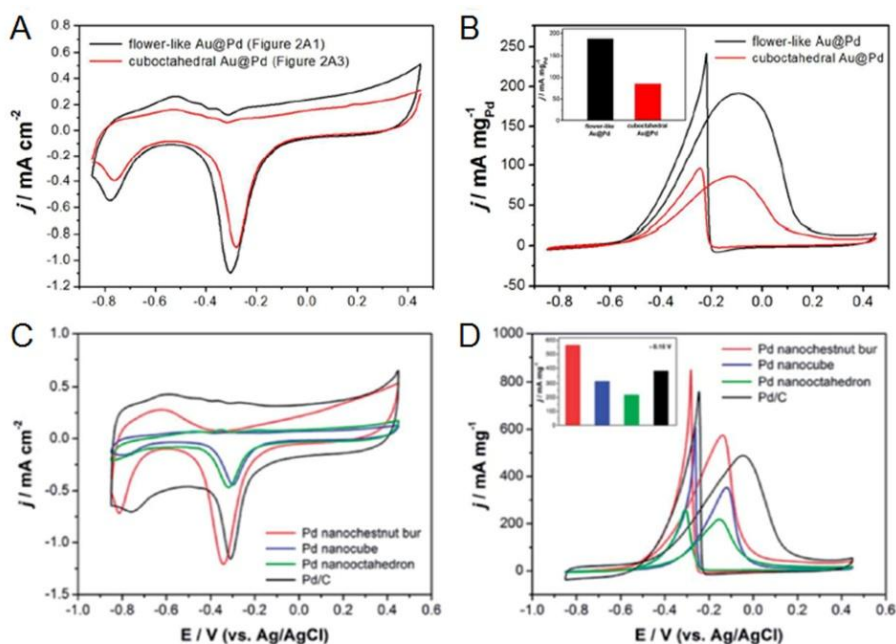


Fig. 10 Electrochemical measurements of glassy carbon electrode modified with Au@Pd flower-like nanoparticles or Pd chestnut-bur-like nanoparticles. (A) Cyclic voltammograms with Au@Pd flower-like and cuboctahedral Au@Pd nanoparticles in 1 M KOH solution and (B) Current densities normalized with respect to the amount of Pd loading in 1 M KOH + 0.5 M ethanol solution. (Reproduced with permission from ref. Kim 2013, copyright 2013 Royal Society of Chemistry) (C) Cyclic voltammograms with Pd nanoparticles with different shapes in 0.1 M KOH solution and (D) Current densities normalized with respect to the amount of Pd loading in 0.1 M KOH + 0.1 M ethanol solution. (Reproduced with permission from ref. Ye 2014, copyright 2014 Royal Society of Chemistry)

#### 4.2 Catalytic applications

Noble metals have been widely used as catalysts in various chemical reactions and industries. Among the noble metals, Pd and Pt are very attractive for catalytic applications due to their exceptional catalytic activity in many organic chemical reactions and electrochemical reactions, such as the oxidation reaction in fuel cells, hydrogenation/dehydrogenation reaction, petroleum cracking, and carbon-carbon bond formation reactions (Zhang 2013 and Chen 2009). Since the catalytic properties are strongly related to the active surface atoms as well as their arrangement and structure, the size- and shape-control of the metal nanoparticles can highly contribute to the enhancement of catalytic properties (Zhou 2009).

The flower-like Au@Pd nanoparticles and the chestnut-bur-like Pd nanoparticles showed excellent electrocatalytic properties toward the ethanol oxidation reaction (Fig. 10) (Kim 2013 and Ye 2014). Both nanoparticles had a high electrochemically active surface area (ECSA), as determined by cyclic voltammograms (CVs) (Fig. 10 A and 10C). The current densities with the flower-like Au@Pd and chestnut-bur-like nanoparticles in the presence of ethanol were also higher than those with nanoparticles having conventional polyhedral shapes. This is because of their highly opened nano-scale structure and large surface areas compared to the conventional polyhedral nanoparticles, which thus they provided more electrochemically active sites. In addition, nanoparticles with these highly opened structures often possess high-index facets along their arms, which have relatively high surface energies and can serve as highly active sites for the reaction. Possible high-index facets along the Pd arms in the flower-like Au@Pd and chestnut-bur-like Pd nanostructures could also play a part in the enhanced catalytic activities toward the ethanol electrooxidation reaction.

#### 4.3 Biological applications

Compared to other noble metals, Au nanoparticles have a remarkable advantage in bio-compatibility and stability. Therefore, Au nanoparticles are popularly used in biological applications, such as biodiagnosis, cell imaging, and photothermal therapy (Murphy 2008 and

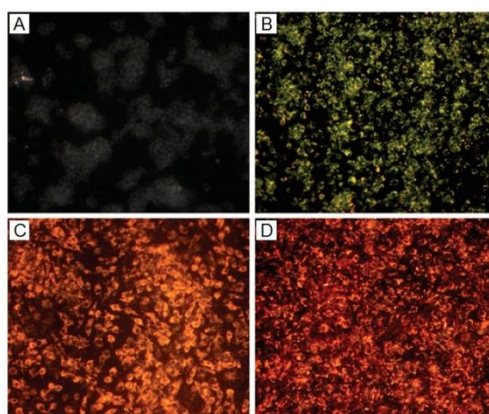


Fig. 11 Dark-Field light scattering images of (A) macrophage cells (RAW 264.7) only and macrophage cells with (B) Au truncated octahedra, (C) rhombic dodecahedra, and (D) octahedra. (Reproduced with permission from ref. Kim 2010, copyright 2009 Royal Society of Chemistry)

Huang 2006). For example, Fig. 11 shows the dark-field light scattering images of macrophage cells with different shapes of Au nanoparticles (Kim 2009). The macrophage cells without Au nanoparticles exhibited only a meager monochrome contrast, whereas those with Au nanoparticles could be clearly recognized with distinct colors due to the strong light scattering signals. Moreover, the color of the enhanced scattering signal was apparently different for each shape of Au nanoparticles, which can be attributed to the dependence of the LSPR wavelength on the shape of Au nanoparticles.

#### 4.4 Templates for further applications

The size- and shape-controlled metal nanoparticles can be also used as templates and building blocks. Those metal nanoparticles provide a well-defined structure and thus their products can be employed in functional devices and complex systems. They can also exhibit additional functions and properties based on the structural change or hybridization with other materials. For example, Skrabalak et al. reported the synthesis of Au nanocages with a hollow structure inside, which was obtained by using Ag nanocubes as a sacrificial template *via* galvanic replacement (Skrabalak 2008). The Au nanocages revealed exceptional optical properties and functionalities resulting from their hollow structure.

Using size-controlled Ag nanoparticles as a sacrificial template, hollow silica particles could be also prepared for a low-reflection coating (Park 2011). First, 30-nm Ag nanoparticles were synthesized with uniform size through the polyol reduction, taking advantage of solvent viscosity (Fig.12A). Then, a silica shell was coated on each Ag nanoparticle *via* the Stöber method (Fig. 12B). For the hollow structure, the Ag nanoparticle in the center of the particle was selectively removed by using diluted nitric acid (Fig. 12C). It should be emphasized that the size of the Ag

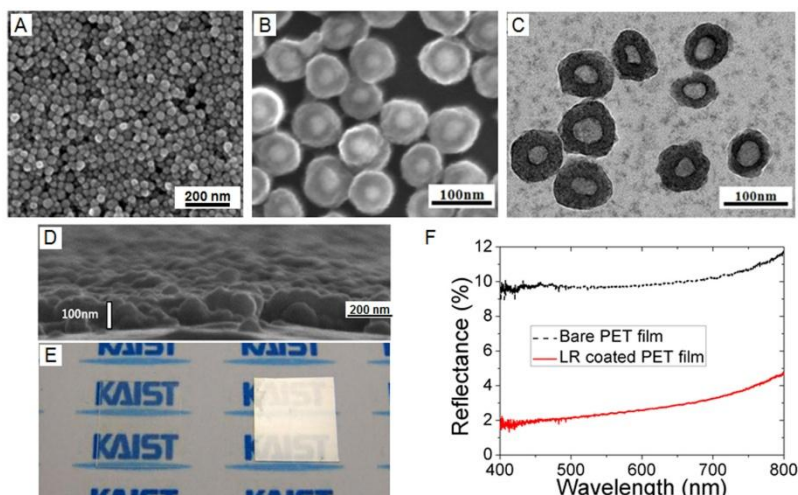


Fig. 12 SEM images of (A) 30-nm Ag nanoparticles and (B) silver-silica core-shell nanoparticles. (C) TEM image of hollow silica particles. (D) SEM cross-sectional image of low-reflection coated on PET film. (E) Optical image of low-reflection coated PET film (left) and bare PET film (right). (F) Reflectance of low-reflection coated on PET film and bare PET film. (Reproduced with permission from ref. Park 2011, copyright 2011 Institute of Physics Publishing)

nanoparticles and their uniformity were very important for the low-reflection coating. The size of Ag nanoparticle should be around 30-nm because a hollow particle larger than 100-nm in size could cause partial scattering of the light and haze. Moreover, if the size of the hollow particles were not uniform, it could be a potential point defect during the low-reflection coating process. Fig. 12D and 12E show the low-reflection coated PET films using the obtained hollow silica nanoparticles, which was uniformly coated on a PET substrate and is clearly transparent without any optical haze. The refractive index of the hollow silica nanoparticles are directly related to the reflectance of the low-reflection coating film. It was confirmed that the reflectance of the low-reflection coated PET film with hollow silica nanoparticles could greatly reduce the reflectance to 70 - 80% compared to the bare PET film (Fig. 12F).

## 5. Conclusions

The synthesis of size- and shape-controlled metal nanoparticles has been presented with several examples of recent research. The strategies and methods to synthesize the size- and shape-controlled metal nanoparticles were introduced with their growth mechanisms. It is illustrated how the properties of metal nanoparticles could be finely characterized and tuned by controllably manipulating their size and the shape. The obtained size- and shape-controlled metal nanoparticles could be used in various fields of applications for optics, electronics, catalysis, biomedical applications, and other functional materials. It is believed that this discussion can offer insights for understanding the size- and shape-controlled synthesis of metal nanoparticles and thus the means to accomplish desirable properties and applications.

## Acknowledgments

This work was supported by grant No. EEWS-2014-N01140052 from EEWS Research Project of the KAIST EEWS Research Center (EEWS: Energy, Environment Water and Sustainability).

## References

- Aiken III, J.D. and Finke, R.G. (1999), "A review of modern transition-metal nanoclusters: Their synthesis, characterization, and applications in catalysis", *J. Mol. Catal. A*, **145**(1), 1-44.
- Aricò, A.S., Bruce, P., Scrosati, B., Tarascon, J.-M. and van Schalkwijk, W. (2005), "Nanostructured materials for advanced energy conversion and storage devices", *Nature Mater.*, **4**(5), 366-377.
- Banfield, J.F., Welch, S.A., Zhang, H., Ebert, T.T. and Penn, R.L. (2000), "Aggregation-Based crystal growth and microstructure development in natural iron oxyhydroxide biomineralization products", *Sci.*, **289**(5480), 751-754.
- Burda, C., Chen, X., Narayanan, R. and El-Sayed, M.A. (2005), "Chemistry and properties of nanocrystals of different shapes", *Chem. Rev.*, **105**(4), 1025-1102.
- Chen, J., Lim, B., Lee, E.P. and Xia, Y. (2009), "Shape-Controlled synthesis of platinum nanocrystals for catalytic and electrocatalytic applications", *Nano Today*, **4**(1), 81-95.
- Choi, K.W., Kim, D.Y., Zhong, X.-L., Li, Z.-Y., Im, S.H. and Park, O.O. (2013), "Robust synthesis of gold rhombic dodecahedra with well-controlled sizes and their optical properties", *Cryst. Eng. Comm.*, **15**(2), 252-258.

- Daniel, M.-C. and Astruc, D. (2004), "Gold nanoparticles: Assembly, supramolecular chemistry, quantum-size-related properties, and applications toward biology, catalysis, and nanotechnology", *Chem. Rev.*, **104**(1), 293-346.
- Dutilleul, M.C., Seisenbaeva, G. and Kessler, V.G. (2014), "Novel solvothermal approach to hydrophilic nanoparticles of late transition elements and its evaluation by nanoparticle tracking analysis", *Adv. Nano Res.*, **2**(2), 77-88.
- Herrero, E., Buller, L.J. and Abruña, H.D. (2001), "Underpotential deposition at single crystal surfaces of Au, Pt, Ag and other materials", *Chem. Rev.*, **101**(7), 1897-1930.
- Huang, X., El-Sayed, I. H., Qian, W., El-sayed, M.A. (2006), "Cancer cell imaging and photothermal therapy in the near-infrared region by using gold nanorods", *J. Am. Chem. Soc.*, **128**(6), 2115-2120.
- Jain, P.K., Lee, K.S., El-Sayed, I.H. and El-Sayed, M.A. (2006), "Calculated absorption and scattering properties of gold nanoparticles of different size, shape, and composition: Applications in biological imaging and biomedicine", *J. Phys. Chem. B*, **110**(14), 7238-7248.
- Jana, N.R., Gearheart, L. and Murphy, C.J. (2001), "Seed-Mediated growth approach for shape-controlled synthesis of spheroidal and rod-like gold nanoparticles using a surfactant template", *Adv. Mater.*, **13**(18), 1389-1393.
- Jana, N.R., Gearheart, L. and Murphy, C.J. (2001), "Wet chemical synthesis of high aspect ratio cylindrical gold nanorods", *J. Phys. Chem. B*, **105**(19), 4065-4067.
- Jin, R., Cao, Y., Mirkin, C.A., Kelly, K.L., Schatz, G.C. and Zheng, J.G. (2001), "Photoinduced conversion of silver nanospheres to nanoprisms", *Science*, **294**(5548), 1901-1903.
- Kenipp, K. (2007), "Surface-Enhanced Raman Scattering", *Phys. Today*, **60**(11), 40.
- Kim, D.Y., Choi, K.W., Im, S.H., Park, O.O., Zhong, X.-L. and Li, Z.-Y. (2012), "One-pot synthesis of gold trisoctahedra with high-index facets", *Adv. Mater. Res.*, **1**(1), 1-12.
- Kim, D.Y., Choi, K.W., Zhong, X.-L., Li, Z.-Y., Im, S.H. and Park, O.O. (2013), "Au@Pd core-shell nanocubes with finely-controlled sizes", *CrystEngComm*, **15**(17), 3385-3391.
- Kim, D.Y., Im, S.H., Lim, Y.T. and Park, O.O. (2010), "Evolution of gold nanoparticles through Catalan, Archimedean, and Platonic solids", *Cryst. Eng. Comm.*, **12**(1), 116-121.
- Kim, D.Y., Im, S.H. and Park, O.O. (2010), "Synthesis of tetrahedral gold nanocrystals with high-index facets", *Cryst. Growth Des.*, **10**(8), 3297-3834.
- Kim, D.Y., Kang, S.W., Choi, K.W., Choi, S.W., Han, S.W., Im, S.H. and Park, O.O. (2013), "Au@Pd nanostructures with tunable morphologies and sizes and their enhanced electrocatalytic activity", *Cryst. Eng. Comm.*, **15**(35), 7113-7120.
- Kim, D.Y., Li, W., Y. Ma, Yu, T., Li, Z.-Y., Park, O.O. and Xia, Y. (2011), "Seed-mediated synthesis of gold octahedra in high purity and with well-controlled sizes and optical properties", *Chem. Eur. J.*, **17**(17), 4759-4764.
- Kim, D.Y., Yu, T., Cho, E.C., Ma, Y., Park, O.O. and Xia, Y. (2011), "Synthesis of gold nano-hexapods with controllable arm lengths and their tunable optical properties", *Angew. Chem. Int. Ed.*, **50**(28), 6328-6331.
- Kelly, K.L., Coronado, E., Zhao, L.L. and Schatz, G.C. (2003), "The optical properties of metal nanoparticle: The influence of size, shape, and dielectric environment", *J. Phys. Chem. B*, **107**(3), 668-677.
- LaMer, V.K. and Dinegar, R.H. (1950), "Theory, production and mechanism of formation of monodispersed hydrosols", *J. Am. Chem. Soc.*, **72**(11), 4847-4854.
- Li, J., Zheng, Y., Zeng, J. and Xia, Y. (2012), "Controlling the size and morphology of Au@Pd core-shell nanocrystals by manipulating the kinetics of seeded growth", *Chem. Eur. J.*, **18**(26), 8150-8156.
- Lim, B., Jiang, M., Yu, T., Camargo, P.H.C. and Xia, Y. (2010), "Nucleation and growth mechanisms for Pd-Pt bimetallic nanodendrites and their electrocatalytic properties", *Nano Res.*, **3**(2), 69-80.
- Lim, B. and Xia, Y. (2010), "Metal nanocrystals with highly branched morphologies", *Angew. Chem. Int. Ed.*, **50**(1), 76-85.
- Lim, B., Xiong, Y. and Xia, Y. (2007), "A water-based synthesis of octahedral, decahedral, and icosahedral Pd nanocrystals", *Angew. Chem. Int. Ed.*, **46**(48), 9279-9282.

- Lu, X., Rycenga, M., Skrabalak, S.E., Wiley, B. and Xia, Y. (2009), "Chemical synthesis of novel plasmonic nanoparticles", *Annu. Rev. Phys. Chem.*, **60**, 167-192.
- Ma, Y., Zeng, J., Li, W., McKiernan, M., Xie, Z. and Xia, X. (2010), "Seed-Mediated synthesis of truncated gold decahedrons with a AuCl/oleylamine complex as precursor", *Adv. Mater.*, **22**(17), 1930-1934.
- Marks, L.D. (1994), "Experimental studies of small particle structures", *Rep. Prog. Phys.*, **57**(6), 603-649.
- Murphy, C.J., Gole, A.M., Stone, J. W., Sisco, P.N., Alkilany, A.M., Goldsmith, E.C. and Baxter, S.C. (2008), "Gold nanoparticles in biology: beyond toxicity to cellular imaging", *Acc. Chem. Res.*, **41**(12), 1721-1730.
- Ni, C., Hassan, P.A. and Kaler, E.W. (2005), "Structural characteristics and growth of pentagonal silver nanorods prepared by a surfactant method", *Langmuir*, **21**(8), 3334-3337.
- Orendorff, C.J. and Murphy, C.J. (2006), "Quantitation of metal content in the silver-assisted growth of gold nanorods", *J. Phys. Chem. B*, **110**(9), 3990-3994.
- Park, K.H., Im, S.H. and Park, O.O. (2011), "The size control of silver nanocrystals with different polyols and its application to low-reflection coating materials", *Nanotechnology*, **22**(4), 045602(6pp).
- Peng, X., Wickham, J. and Alivisatos, A.P. (1998), "Kinetics of II-VI and III-V colloidal semiconductor nanocrystals growth: "Focusing" of size distribution", *J. Am. Chem. Soc.*, **120**(21), 5343-5344.
- Pimpinelli, A. and Villain, J. (1998), *Physics of Crystal Growth*, Cambridge University Press: Cambridge, UK.
- Qiu, P. and Mao, C. (2009), "Seed-Mediated shape evolution of gold nanomaterials: from spherical nanoparticles to polycrystalline nanochains and single-crystalline nanowires", *J. Nanopart. Res.*, **11**(4), 885-894.
- Rosi, N.L. and Mirkin, C.A. (2005), "Nanostructures in biodiagnostics", *Chem. Rev.*, **105**(4), 1547-1562.
- Rycenga, M., Cobley, C. M., Zeng, J., Li, W., Moran, C. H., Zhang, Q., Qin, D. and Xia, Y. (2011), "Controlling the synthesis and assembly of silver nanostructures for plasmonic applications", *Chem. Rev.*, **111**(6), 3669-3712.
- Sau, T.K. and Murphy, C.J. (2004), "Room temperature, high-yield synthesis of multiple shapes of gold nanoparticles in aqueous solution", *J. Am. Chem. Soc.*, **126**(28), 8648-8649.
- Sau, T.K., Rogach, A.L., Jäckel, F., Klar, T.A. and Feldmann, J. (2009), "Properties and applications of colloidal nonspherical noble metal nanoparticles", *Adv. Mater.*, **22**(16), 1805-1825.
- Seo, D., Park, J.C. and Song, H. (2006), "Polyhedral gold nanocrystals with  $O_h$  symmetry: from octahedral to cubes", *J. Am. Chem. Soc.*, **128**(46), 14863-14870.
- Seo, D., Yoo, C.I., Chung, I.S., Park, S.M., Ryu, S. and Song, H. (2008), "Shape adjustment between multiply twinned and single-crystalline polyhedral gold nanocrystals: decahedra, icosahedra, and truncated tetrahedral", *J. Phys. Chem. C*, **112**(7), 2469-2475.
- Skrabalak, S.E., Chen, J., Sun, Y., Lu, X., Au, L., Cobley, C.M. and Xia, Y. (2008), "Gold nanocages: Synthesis, properties, and applications", *Acc. Chem. Res.*, **41**(12), 1587-1595.
- Somorjai, G.A. (1985), "Surface science and catalysis", *Science*, **227**(4689), 902-908.
- Sun, Y., Mayers, B., Herricks, T. and Xia, Y. (2003), "Polyol synthesis of uniform silver nanowires: A plausible growth mechanism and the supporting evidence", *Nano Lett.*, **3**(7), 955-960.
- Sun, Y., Mayers, B. and Xia, Y. (2003), "Transformation of silver nanospheres into nanobelts and triangular nanoplates through a thermal process", *Nano Lett.*, **3**(5), 675-679.
- Sun, Y. and Xia, Y. (2003), "Triangular nanoplates of silver: Synthesis, characterization, and use as sacrificial template for generating triangular nanorings of gold", *Adv. Mater.*, **15**(9), 695-699.
- Tao, A.R., Habas, S. and Yang, P. (2008), "Shape control of colloidal metal nanocrystals", *Small*, **4**(3), 310-325.
- Tian, N., Zhou, Z.-Y., Sun, S.-G., Ding, Y. and Wang, Z.L. (2007), "Synthesis of tetrahedral platinum nanocrystals with high-index facets and high electro-oxidation activity", *Science*, **316**(5825), 732-735.
- Vicsek, T. (1992), *Fractal Growth Phenomena*, 2nd ed., World Scientific, Singapore.
- Wang, D.H., Kim, D.Y., Choi, K.W., Seo, J.H., Im, S.H., Park, J.H., Park, O.O. and Heeger, A.J. (2011), "Enhancement of donor-acceptor polymer bulk heterojunction solar cell power conversion efficiencies by addition of Au nanoparticles", *Angew. Chem. Int. Ed.*, **50**(24), 5519-5523.

- Wang, Y., Yan, B. and Chen, L. (2013), "SERS tags: Novel optical nanoprobe for bioanalysis", *Chem. Rev.*, **113**(3), 1391-1428.
- Wang, Z.L. (2000), "Transmission electron microscopy of shape-controlled nanocrystals and their assemblies", *J. Phys. Chem. B*, **104**(6), 1153-1175.
- Washio, I., Xiong, Y. and Xia, Y. (2006), "Reduction by the end groups of poly(vinyl pyrrolidone): A new and versatile route to the kinetically controlled synthesis of Ag triangular nanoplates", *Adv. Mater.*, **18**(13), 1745-1749.
- Wilcoxon, J.P. and Abrams, B.L. (2006), "Synthesis, structure and properties of metal nanoclusters", *Chem. Soc. Rev.*, **35**(11), 1162-1194.
- Wiley, B.J., Im, S.H., Li, Z.Y., McLellan, J., Siekkinen, A. and Xia, Y. (2006), "Maneuvering the surface plasmon resonance of silver nanostructures through shape-controlled synthesis", *J. Phys. Chem. B*, **110**(32), 15666-15675.
- Xia, Y., Xiong, Y., Lim, B. and Skrabalak, S.E. (2009), "Shape-Controlled synthesis of metal nanocrystals: Simple chemistry meets complex physics?", *Angew. Chem. Int. Ed.*, **48**(1), 60-103.
- Xiong, Y., Cai, H., Wiley, B.J., Wang, J., Kim, M.J. and Xia, Y. (2007), "Synthesis and mechanistic study of palladium nanobars and nanorods", **129**(12), 3665-3675.
- Xiong, Y., McLellan, J. M., Chen, J., Yin, Y., Li, Z.-Y. and Xia, Y. (2005), "Kinetically controlled synthesis of triangular and hexagonal nanoplates of palladium and their SPR/SERS properties", *J. Am. Chem. Soc.*, **127**(48), 17118-17127.
- Xiong, Y., Siekkinen, A.R., Wang, J., Yin, Y., Kim, M.J. and Xia, Y. (2007) "Synthesis of silver nanoplates at high yields by slowing down the polyol reduction of silver nitrate with polyacrylamide", *J. Mater. Chem.*, **17**(25), 2600-2602
- Xiong, Y., Wiley, B. J. and Xia, Y. (2007), "Nanocrystals with unconventional shapes- A class of promising catalyst", *Angew. Chem. Int. Ed.*, **46**(38), 7157-7159.
- Xiong, Y. and Xia, Y. (2007), "Shape-Controlled synthesis of metal nanostructure: The case of palladium", *Adv. Mater.*, **19**(20), 3385-3391.
- Ye, S.J., Kim, D.Y., Kang, S.W., Choi, K.W., Han, S.W. and Park, O.O. (2014), "Synthesis of chestnut-bur-like palladium nanostructures and their enhanced electrocatalytic activities for ethanol oxidation", *Nanoscale*, **6**(8), 4182-4187.
- Zhang, H., Jin, M. and Xia, Y. (2012), "Noble-Metal nanocrystals with concave surfaces: Synthesis and applications", *Angew. Chem. Int. Ed.*, **51**(31), 7656-7673.
- Zhang, H., Jin, M., Xiong, Y., Lim, B. and Xia, Y. (2013), "Shape-Controlled synthesis of Pd nanocrystals and their catalytic applications", *Acc. Chem. Res.*, **46**(8), 1783-1794.
- Zheng, H., Smith, R.K., Jun, Y.-W., Kisielowski, C., Dahmen, U. and Alivisatos, A.P. (2009), "Observation of single colloidal platinum nanocrystal growth trajectories", *Science*, **324**(5932), 1309-1312.
- Zhou, Z.-Y., Tian, N., Huang, Z.Z., Chen, D.-J. and Sun, S.-G. (2008), "Nanoparticle catalyst with high energy surface and enhanced activity synthesized by electrochemical method", *Faraday Discuss.*, 2009, **140**, 81-92.